REVIEW OF NASA SUPERCRITICAL AIRFOILS

Richard T. Whitcomb
National Aeronautics and Space Administration
Langley Research Center
Hampton, Virginia 23665 USA

Abstract

NASA supercritical airfoils are characterized by a substantially reduced curvature of the mid-chord region of the upper surface together with increased camber near the trailing edge. The basic aerodynamic phenomena associated with the airfoils and representative wind tunnel results are discussed. The results indicate that the drag rise Mach numbers for NASA supercritical airfoils are 0.1 higher than for comparable NACA 6-series airfoils. A recent analytic method for predicting the aerodynamic characteristics of supercritical airfoils is described. The flight demonstration programs of three applications of supercritical airfoils utilizing the F-8, T-2C and F-111 as test beds are summarized.

I. Introduction

It is well known that the subsonic cruise speeds of high performance aircraft are limited by the onset of the transonic drag rise. The use of wing sweepback delays this onset. However, for practical amounts of sweepback (approximately 35°) the onset still occurs well below the speed of sound (Mach numbers between 0.80 and 0.85). One method for increasing the cruise speed further is the use of airfoil shapes which delay the drag rise.

The first airfoils developed in the USA to delay the drag rise were the NACA 1 series.[1] These airfoils, designed to increase the critical Mach number, that is, the Mach number at which supersonic flow first develops locally on the airfoil, have drag rise Mach numbers significantly higher than the earlier NACA four digit series airfoils. However the low-speed, high-lift characteristics of these airfoils are significantly poorer than for the earlier airfoils. As a result they are used only on high speed propeller blades. The NACA 6-series airfoils also provide increased critical Mach numbers with resulting improvements in the drag rise characteristics as compared with those for the 4-digit series.[2] They result in a small degradation in the low speed characteristics. These airfoils, or their derivatives, were used on most of the first generation of subsonic jet aircraft designed in the USA.

The first airfoils designed specifically to delay drag rise by improving the supercritical flow above the upper surface were the "peaky" airfoils of Pearcy.[3] They provide an isentropic recompression of the supersonic flow ahead of the shock wave located on the forward region of the airfoil. These airfoils result in approximately a .02 to .03 delay in the drag rise with a small degradation of the low speed characteristics compared with NACA 6-series airfoils. These airfoils or their derivatives were used on the second generation of subsonic jet aircraft designed in the USA.

The airfoils to be described herein also are designed to improve the supercritical flow. They are designed to allow the shock wave to move to the rear part of the airfoil at the design condition. As a result they provide considerably higher drag rise Mach numbers than previous airfoils. In the first work on this approach[4] it was assumed that a slot was required to stabilize the upper surface boundary layer. Later it was found that with the proper upper surface pressure distribution the boundary layer could be maintained attached up to the design Mach number without the slot. The results of the first work on the integral or unslotted airfoil was given limited distribution in 1967 in a Confidential Langley Working Paper. This paper has been declassified recently and forms the basis for much of the discussion included herein. It should be noted, however, that the extensive experimental results obtained since 1967 on refinements and applications of the NASA supercritical airfoils are still classified.

II. Description and Flow Phenomena at Design Condition

Description

The evolution of the general shape of the NASA supercritical airfoil is shown in figure 1. In all cases the shape is characterized by substantially reduced curvature of the middle region of the upper surface with a large amount of camber near the trailing edge. Also the leading edge radius is larger than previously used and the trailing edge closure angle is very small. It will be noted that the original integral airfoil had a very thin trailing edge which led to structural problems. Therefore the trailing edge was thickened as shown at the bottom of figure 1. This change improved not only the structure but also the high speed aerodynamic characteristics at lifting conditions with very little increase in the basic subsonic drag level. The advantages of thickened trailing edges for transonic airfoils is discussed in reference 5. The airfoils used for all the flight demonstration programs to be described have included this thickened trailing edge.

Flow Phenomena at Design Condition

A comparison of the supercritical flow phenomena for the NASA supercritical airfoil and an NACA 6-series airfoil at the cruise lift coefficient is presented in figure 2. For the NACA 6-series airfoil, as shown at the top of the figure, the supersonic flow accelerated to the shock wave located near the mid-chord, causing a strong, extensive shock wave. This wave is followed immediately by a subsonic pressure recovery to the trailing edge. The energy loss in the shock causes some drag increase. However, the dominant problem is severe boundary separation caused by the large, steep total streamwise pressure increase. This separation, of course, produces the well known abrupt drag rise, buffeting, and stability problems.

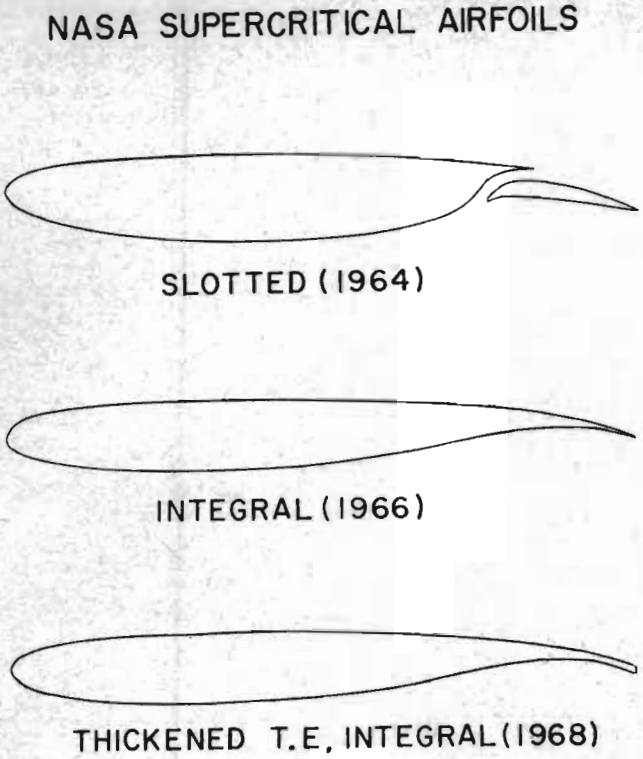

FIGURE 1

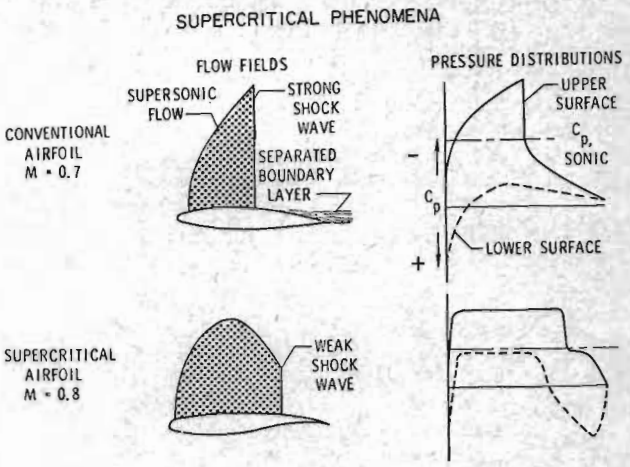

FIGURE 2

The surface pressure distribution and flow field shown at the bottom of figure 2 are representative of those obtained for NASA supercritical airfoils. The upper surface pressure and related velocity distributions are characterized by a shock location significantly aft of the midchord, an approximately uniform supersonic velocity from about the 5% chord station to the shock, a plateau in the pressure distribution rearward of the shock, a relatively steep subsonic pressure recovery on the extreme rearward region, and a trailing edge pressure near ambient. The lower surface has roughly constant negative pressure coefficients corresponding to subcritical velocities over the forward region and a rapid increase in pressure rearward of the midchord to a substantially positive pressure forward of the trailing edge.

The elimination of the flow acceleration on the upper surface ahead of the shock wave, which results primarily from the reduced curvature of the midchord region, obviously provides a reduction of the Mach number ahead of the shock for a given lift coefficient with a resulting decrease of the shock strength. The strength and extent of the shock at the design condition can be reduced below that for the pressure distribution shown by shaping the airfoil to provide a gradual deceleration of the supersonic flow from near the leading edge to the shock wave.[3], [4], [6] However, as will be discussed in Section IV, such a shape may have an increased drag at lower Mach numbers. Extensive experiments indicate that the shape associated with the design point distribution shown provides acceptable drag values over the Mach number and lift coefficient range.

The plateau in the pressure distribution rearward of the shock wave allows a reenergization of the boundary layer by mixing after it moves through the severe adverse pressure gradient of the shock and before it moves through the pressure gradient near the trailing edge. As a result, the boundary layer can move through a greater total pressure rise without separating. The importance of this effect is shown by the experimental data presented in Section IV. The near-ambient pressure at the trailing edge, which results from the small included angle of the trailing edge, reduces to a minimum the total pressure rise the upper surface boundary layer must traverse and thus minimizes the tendency toward separation.

The maintainence of subcritical flow over the forward region of the lower surface eliminates the possibility of a shock wave on that surface. The pressure rise of a possible shock wave superimposed on the pronounced pressure rise on the rear portion of this surface would greatly increase the tendency for the boundary layer to separate. The streamwise pressure increase rearward of the midchord is defined by the Stratford criteria.[7] The substantially positive pressure on the rear part of the lower surface, associated with the surface concavity of this region, provides a substantial increase in the circulation around the airfoil with a resulting reduction in the angle of attack required to achieve the design lift coefficient. Usually this angle is slightly negative (about -0.5°). With this negative angle of attack the crest (the maximum vertical coordinate with respect to the free airstream) of the upper surface is near the midchord. This factor together with the reduced curvature of the midregion of the upper surface, results in favorable chordwise forces associated with the supersonic flow region, even with the rearward shock location. The significance of the distribution of the chordwise forces for supercritical flow is discussed in reference 3.

Theory and experiments indicate that with the upper surface pressure distribution shown and at the negative angle of attack required to obtain the design lift coefficient the vertical extent of the supersonic field decreases ahead of the shock wave as shown on the left in figure 2. This effect is similar to that for airfoils designed specifically to minimize the extent of the shock at the design point[3], [4], [6] although in this case the effect is somewhat smaller. The flow field calculations of reference 6 illustrate the origin of this effect.

The relatively large leading edge radii of the NASA supercritical airfoils allow simultaneous reductions of the curvatures of the midchord regions of both the upper and lower surfaces with resulting reductions of the induced velocities. However, experiments indicate that the use of relative radii larger than that listed in Table I results in increases of the low speed drag.

III. Experiments and Aerodynamic Characteristics

Experiments

The Langley 8-Foot Transonic Pressure Tunnel in which the NASA supercritical airfoils have been developed has solid side walls and thus can be used without modification to obtain two-dimensional results. A model of an integral (unslotted) supercritical airfoil is shown installed in the tunnel in figure 3. The lift and pitching moment characteristics are obtained by surface pressure measurements while the drag is derived from wake surveys. These measurements also provide substantial information on the flow phenomena involved. Additional information on the flow phenomena is obtained by surface oil flow studies.[8] The test Reynolds number at Mach numbers near 0.80 is 7×10^6 which is substantially less than the flight values for most airplanes. To simulate full scale Reynolds numbers at least at and near the design condition the technique described in reference 9 is utilized.

Aerodynamic Characteristics

To provide a general indication of the aerodynamic characteristics of NASA supercritical airfoils at and off the design condition the experimental results for the 11%-thick representative airfoil shape defined by Table I will be presented. The variation of drag with Mach number for the design normal force coefficient of 0.6 is shown in figure 4. (At the low angles of attack for which results are presented herein, the normal force coefficient is approximately equal to the lift coefficient). Similar variations for an NACA 64-212 airfoil[10] and a slotted supercritical airfoil[4] are shown for comparison. All results are corrected to a condition for boundary transition at the 8% chord station. As indicated by figure 5 the supercritical airfoil is structurally equivalent to a NACA 6-series airfoil of a somewhat greater thickness-to-chord ratio. Therefore the data for the 11%-thick supercritical airfoil are compared with the available data for a 12% rather than a 10%-thick NACA 6-series airfoil.

TWO-DIMENSIONAL AIRFOIL MOUNTED IN THE 8-FT TRANSONIC PRESSURE TUNNEL

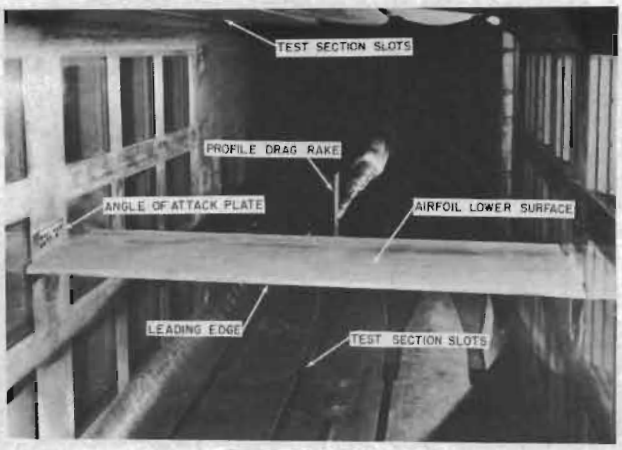

FIGURE 3

The integral supercritical airfoil experiences a small drag increase starting at a Mach number of about 0.7 and an abrupt drag rise associated with boundary layer separation at M = 0.80. (Refinements of the airfoil shapes developed since these data were obtained have essentially eliminated the small drag increase at a cost of an .01 decrease in the drag rise Mach number). For the approximately comparable NACA 6-series airfoil the drag rise starts at a Mach number of about 0.69. The original slotted supercritical airfoil experiences the drag rise at a Mach number just above 0.79. However an analysis of thickness effects indicates that a slotted airfoil 11% thick would experience

TABLE I.- COORDINATES FOR AN 11%-THICK REPRESENTATIVE NASA SUPERCRITICAL AIRFOIL

x/c	z/c	
	Upper surface	Lower surface
0.0075	0.0176	-0.0176
.0125	.0215	-.0216
.0250	.0276	-.0281
.0375	.0316	-.0324
.0500	.0347	-.0358
.0750	.0394	-.0408
.1000	.0428	-.0444
.1250	.0455	-.0472
.1500	.0476	-.0493
.1750	.0493	-.0510
.2000	.0507	-.0522
.2500	.0528	-.0540
.3000	.0540	-.0548
.3500	.0547	-.0549
.4000	.0550	-.0541
.4500	.0548	-.0524
.5000	.0543	-.0497
.5500	.0533	-.0455
.5750	.0527	-.0426
.6000	.0519	-.0389
.6250	.0511	-.0342
.6500	.0501	-.0282
.6750	.0489	-.0215
.7000	.0476	-.0149
.7250	.0460	-.0090
.7500	.0442	-.0036
.7750	.0422	.0012
.8000	.0398	.0053
.8250	.0370	.0088
.8500	.0337	.0114
.8750	.0300	.0132
.9000	.0255	.0138
.9250	.0204	.0131
.9500	.0144	.0106
.9750	.0074	.0060
1.0000	-.0008	-.0013
	L. E. radius: 0.0245c	

COMPARISON OF DRAG-RISE CHARACTERISTICS

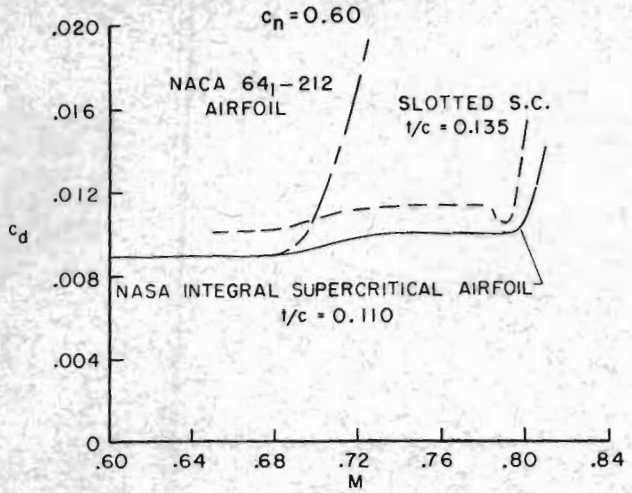

FIGURE 4

a drag rise at about 0.81 or 0.82. Thus the elimination of the slot had a small adverse effect on the drag rise Mach number. The higher drag level for the slotted airfoil of course results from the added skin friction associated with the slot. The dip in the variation of drag with Mach number at a Mach number of 0.79 is due to an essential elimination of the shock wave for this condition.

The variation of the normal force coefficient for separation onset with Mach number is shown in figure 6. It will be noted that the supercritical airfoil provides a greater delay in separation onset compared with the NACA airfoil at the higher normal forces than at the design condition. It also provides a substantial increase in the maximum normal force at these higher Mach numbers. These characteristics of supercritical airfoils would result in a substantial improvement of the

COMPARISON OF CHORDWISE THICKNESS DISTRIBUTIONS

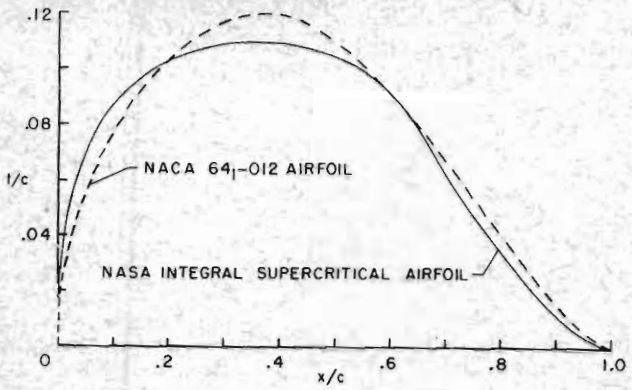

FIGURE 5

COMPARISON OF SEPARATION ONSET

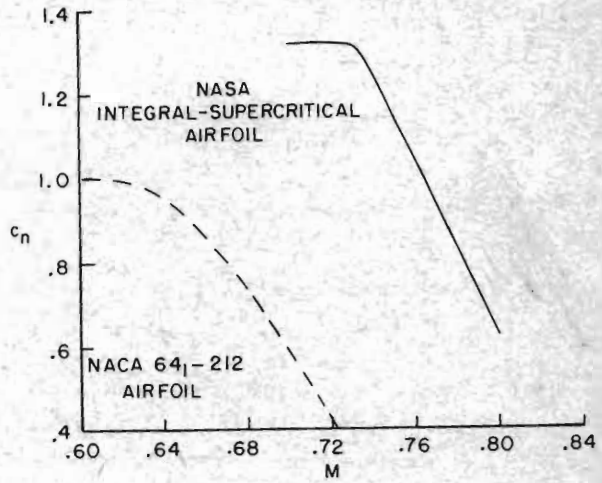

FIGURE 6

maneuverability of fighters at high subsonic speeds. The phenomena associated with this effect will be discussed later.

Because of the increased aft loading on the NASA integral supercritical airfoil, the pitching moments for a given normal force coefficient are substantially more negative than for the NACA 6-series airfoils (figure 7). However, they are significantly less negative than for the original slotted supercritical airfoil. Wind tunnel results obtained for a swept supercritical wing, developed for the flight demonstration program to be discussed later, indicate that the twist required to obtain the proper span load distribution results in a positive pitching moment which approximately offsets the negative pitching moment associated with the section. As a result little or no trim penalty is incurred, at least with such a swept wing.

The variations of drag and pitching moment with normal force coefficients at representative Mach numbers for the 11%-thick representative integral supercritical airfoil are presented in figure 8 for reference.

IV. Flow Phenomena at Off-Design, Subcritical, and High Lift Conditions

The pressure distributions measured on the 11%-thick representative NASA supercritical airfoil defined by Table I provide a general indication of the flow phenomena associated with NASA supercritical airfoils at off-design, subcritical, and high lift conditions (figures 9 - 12). In these figures the circle symbols are upper surface measurements, the squares are lower surface values.

At a Mach number slightly above the design value (figure 9) the shock wave location is rearward of that for the design condition with a small acceleration ahead of the wave. This change causes a slight increase in the shock losses (figure 4) but does not result in boundary layer separation. Separation occurs when the shock wave moves farther rearward and the pressure plateau described in Section II is eliminated.

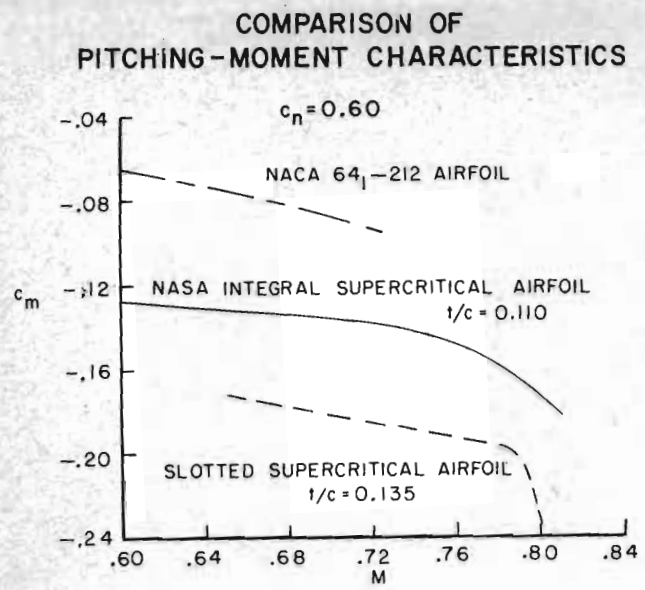

FIGURE 7

At a Mach number just below the design value (figure 10) the shock location is significantly farther forward than for the design condition and the flow experiences a reacceleration rearward of the shock with a supercritical peak velocity near the 75% chord station. This reacceleration causes a substantially greater and steeper pressure increase to the trailing edge as compared with the design condition. This steeper recovery results in a small adverse effect on the trailing edge pressure recovery and drag. For unslotted airfoils designed to achieve a shockless design condition[6] the reacceleration velocity can be sufficiently great to cause a second rearward shock wave.[11] The total pressure rise of this second shock and the immediately following subsonic pressure recovery may cause significant boundary layer separation near the trailing edge.

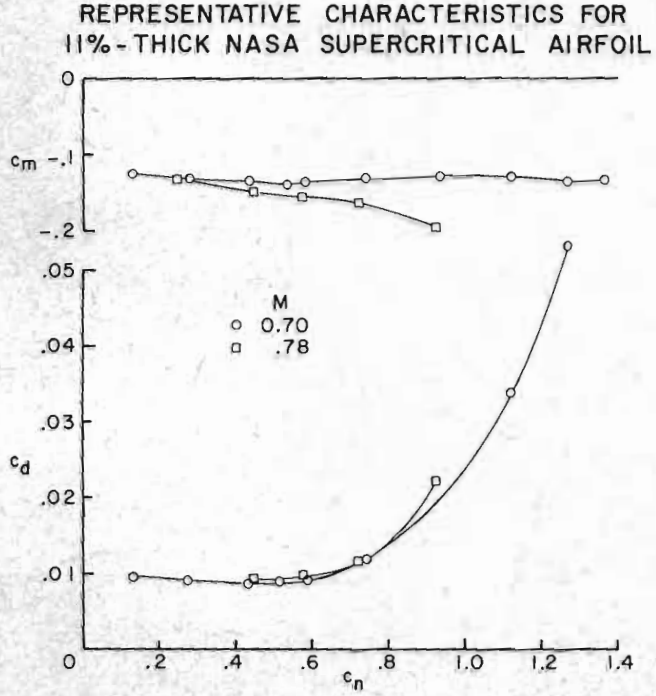

FIGURE 8

At subcritical Mach numbers (figure 11) the pressure distribution has a significant peak near the leading edge. The presence of this peak results in a small drag increment for subcritical and slightly supercritical conditions. If an airfoil is shaped to provide a decelerating supersonic velocity distribution on the upper surface at the design condition as discussed earlier this subcritical peak is substantially greater than that shown with a resulting increase in the drag for the subcritical and slightly supercritical conditions.

The pressure distribution shown in figure 12 is that measured at the high lift corner of the variation of normal force for separation onset with Mach number shown previously in figure 6. The shock wave, associated with a local upstream Mach number of 1.4, causes a very large adverse pressure gradient. However, the trailing edge pressure recovery and a surface oil flow study indicate that the boundary layer does not completely separate. The bulge in the pressure distribution aft of the shock wave and the surface oil study indicate a very large separation bubble under the shock which reattaches near the .75 chord station. For previous airfoil shapes, such as the NACA 6-series, the presence of a shock wave associated with an upstream Mach number of 1.4 causes very severe boundary layer separation.[12] The key to the greater stability of the boundary layer for the supercritical airfoil is the plateau in the pressure distribution aft of the shock wave described in Section II. For previous airfoils the subsonic pressure recovery immediately downstream of the shock wave opposes boundary layer reattachment. With the plateau on the supercritical airfoil this adverse effect is eliminated. It is of interest that unpublished boundary layer surveys indicate that the boundary layer separation development under the shock for supercritical airfoils is quite similar to that on a flat plate.[13]

Experimental results not presented herein indicate that the low speed maximum lift characteristics for NASA supercritical airfoils are also superior to those for comparable NACA 6-series airfoils.

V. Thick Supercritical Airfoils

In the previous discussion the increase in drag rise Mach number for a given airfoil thickness-to-chord ratio provided by the NASA supercritical airfoil has been emphasized. However, the same approach can be used to provide a substantial increase in section thickness-ratio for the same drag rise Mach number. The first thick supercritical airfoil was developed by W. Palmer of the Columbus, Ohio Division of North American-Rockwell (figure 13). This 17%-thick airfoil has the same drag rise Mach number as a 12%-thick NACA 6-series airfoil at the same lift coefficient.

NEAR-DESIGN PRESSURE DISTRIBUTION ON 11%-THICK NASA SUPERCRITICAL AIRFOIL

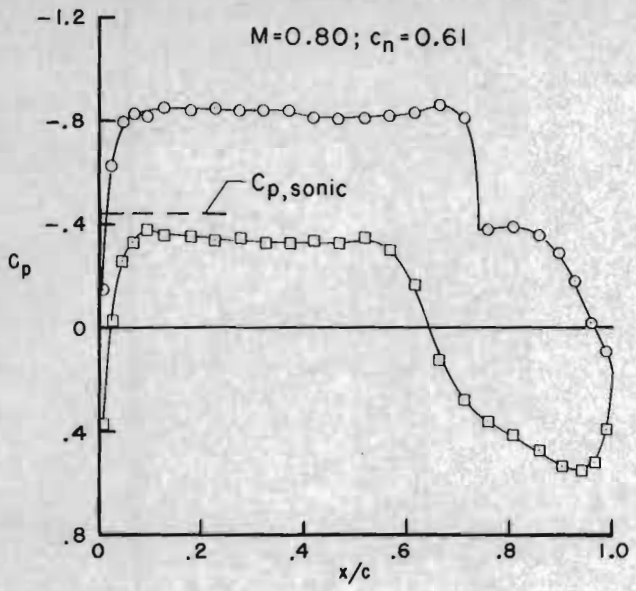

FIGURE 9

SUBCRITICAL PRESSURE DISTRIBUTION ON 11%-THICK NASA SUPERCRITICAL AIRFOIL

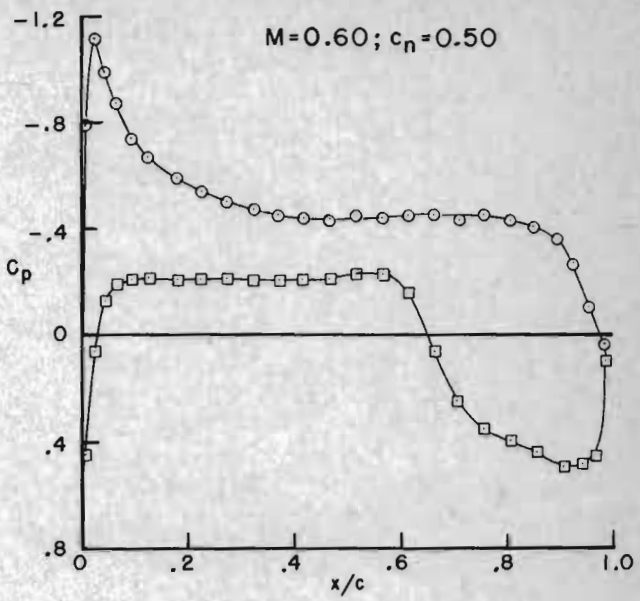

FIGURE 11

OFF-DESIGN PRESSURE DISTRIBUTION ON 11%-THICK NASA SUPERCRITICAL AIRFOIL

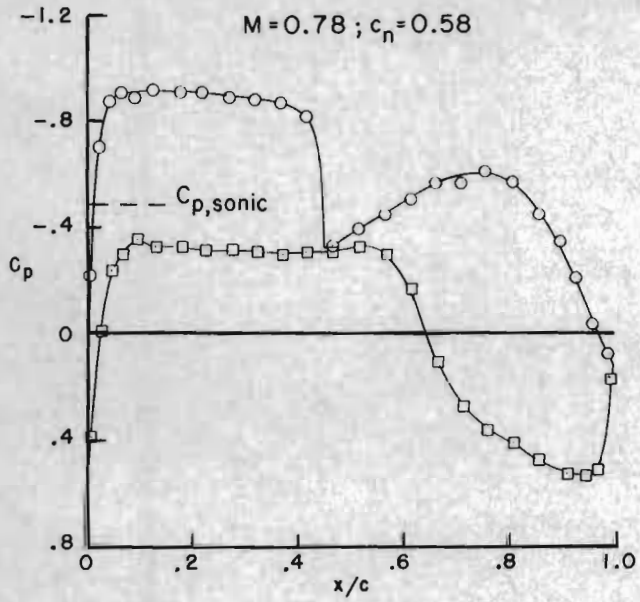

FIGURE 10

HIGH LIFT PRESSURE DISTRIBUTION ON 11%-THICK NASA SUPERCRITICAL AIRFOIL

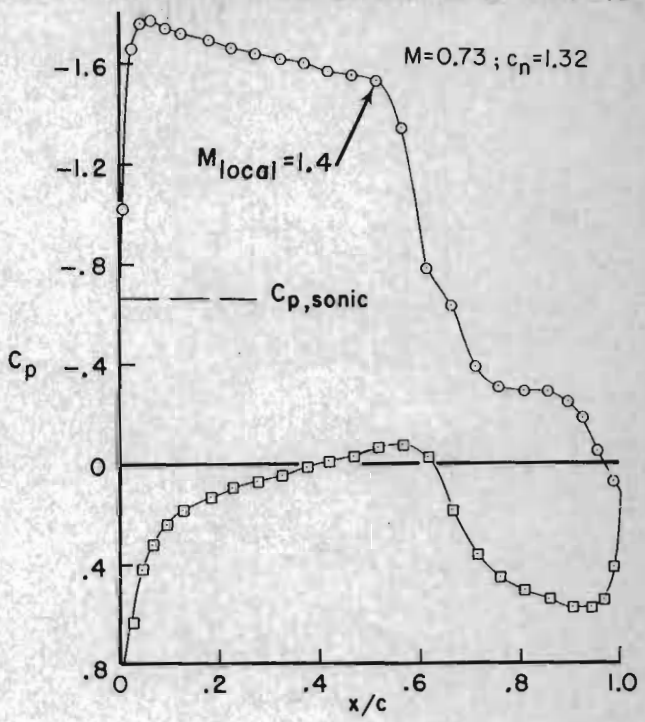

FIGURE 12

VI. Theoretical Analysis

Considerable progress has been made during the last three years in providing theoretical methods for the design and analysis of two-dimensional airfoils at supercritical Mach numbers. No attempt will be made to cover all this work, instead the method being used at Langley in a continuing effort on supercritical airfoils will be described.

The initial comparisons of theoretically derived pressure distributions on NASA supercritical airfoils with experimental results indicate very poor agreement. The differences are associated with the development of the boundary layers on these airfoils, illustrated by figure 14. The

THICK SUPERCRITICAL AIRFOIL
(PALMER OF NORTH AMERICAN ROCKWELL, COLUMBUS)

FIGURE 13

INFLUENCE OF BOUNDARY-LAYER DISPLACEMENT ON EFFECTIVE CAMBER OF SUPERCRITICAL AIRFOIL

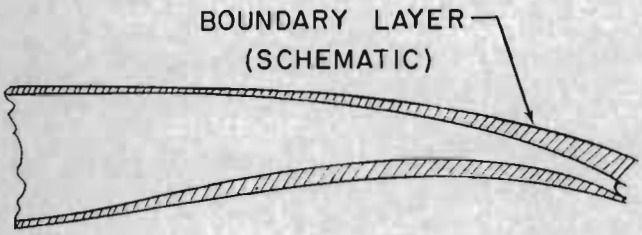

FIGURE 14

CONFORMAL COORDINATE SYSTEM FOR 2-D AIRFOIL CALCULATIONS

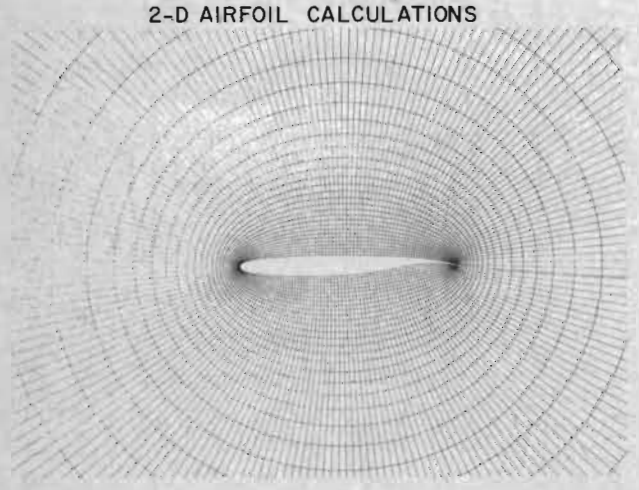

FIGURE 15

VISCOUS EFFECTS ON PRESSURE DISTRIBUTIONS FOR A SUPERCRITICAL AIRFOIL

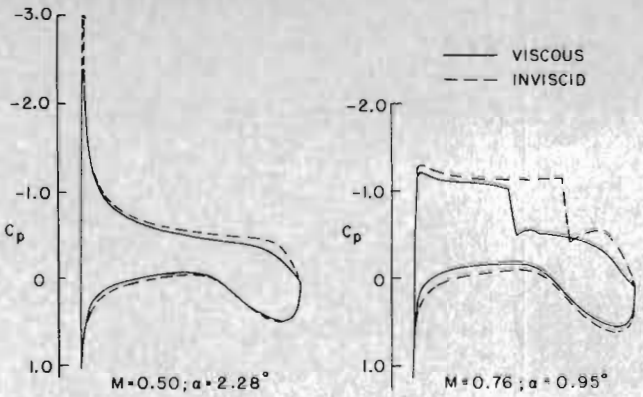

FIGURE 16

steep pressure rise near the trailing edge of the upper surface causes the boundary layer to thicken significantly. On the lower surface the pressure rise from about the .5 to the .9 chords results in a substantial thickening of the boundary layer in the cusp while the rapid pressure decrease near the trailing edge causes a pronounced thinning of the boundary layer. Each of these effects contributes to a substantial reduction of the effective aft camber of the airfoil. It was concluded that for NASA supercritical airfoils any analytic method must include the effect of the boundary layer.

Recently an analytic method which includes the effect of the boundary layer has been developed by Bavitz at Langley.[14] This iterative procedure is based on the method of Korn and Garabedian[15] for analyzing the external supercritical field, which implements a mixed finite-difference scheme related to that of Murman and Cole.[16] A similar method was also developed by Jameson.[17] The coordinate system shown in figure 15, was suggested by Sells[18] and consists of mapping the interior of the unit circle conformally onto the exterior of the airfoil with the point at infinity corresponding to the origin. These flow field computations are made for airfoil shapes modified by the calculated displacement thicknesses of the upper and lower surface boundary layers. The displacement thicknesses are determined by the method of Bradshaw.[19] Since the boundary layer calculations are not applicable near the trailing edge an empirical correction is applied for this region. A similar method has also been developed by Bauer at the Courant Institute.

The effect of including the boundary layer on analytical predicted pressure distributions for an NASA supercritical airfoil is illustrated in figure 16. These comparisons are for lift coefficients substantially greater than the design value. At a subcritical Mach number, including the effect of the boundary layer causes a moderate change in the predicted lift. However, at a supercritical Mach number including the effect of the boundary layer results in substantial changes of the position of the shock wave and the lift. Comparisons

COMPARISON OF EXPERIMENTAL & THEORETICAL PRESSURE DISTRIBUTIONS

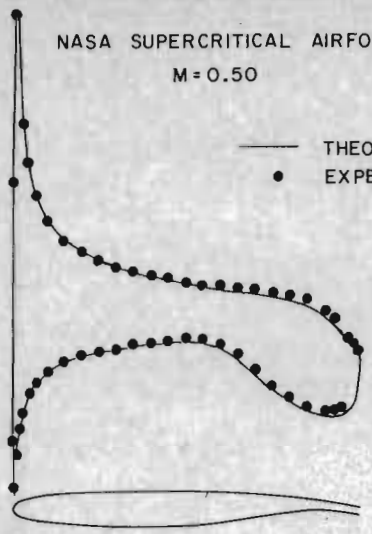

FIGURE 17

COMPARISON OF EXPERIMENTAL & THEORETICAL PRESSURE DISTRIBUTIONS

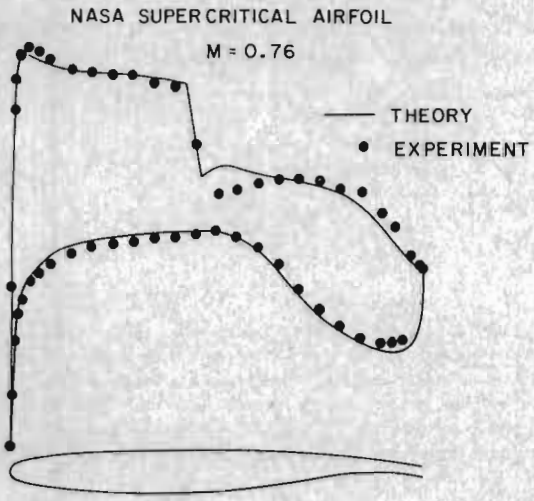

FIGURE 18

of theoretical pressure distributions obtained by this method with experimental distributions for a NASA supercritical airfoil at a subcritical and a supercritical condition are presented in figures 17 and 18 respectively. Again these comparisons are for lift coefficients substantially greater than the design value. In both cases the agreement is quite good. The difference in pressures just rearward of the shock wave for the supercritical condition (figure 18) is due to the fact that the field calculation underpredicts the pressure jump through the shock. Recently Jameson

U.S. NAVY F-8 WITH TRANSPORT TYPE SUPERCRITICAL WING

FIGURE 19

F-8 FLIGHT DEMONSTRATION PROGRAM

WING APPLICATION — LONG RANGE TRANSPORT

OBJECTIVE — INCREASED CRUISE SPEED TO NEAR-SONIC VALUE WITHOUT DEGRADATION OF OFF-DESIGN CHARACTERISTICS

SPONSOR — NASA

F-8 TEST BED — PROVIDED BY U.S. NAVY

CONFIGURATION DESIGN & DEVELOPMENT — NASA LANGLEY

WING STRUCTURAL DESIGN & FABRICATION — NORTH AMERICAN-ROCKWELL, LOS ANGELES

FLIGHT PROGRAM — NASA FLIGHT RESEARCH CENTER

CHRONOLOGY

APPROVAL — 1968
FIRST FLIGHT — 1971
COMPLETION — 1973

CONCLUSION — WIND-TUNNEL RESULTS VERIFIED

FIGURE 20

has solved this problem and the method is now being modified to incorporate his solution. It should be noted that the airfoil shapes shown at the bottom of these figures include the displacement thicknesses of the upper and lower surface boundary layers.

VII. Flight Demonstration Program

Because of the drastically different nature of the flow over the NASA supercritical airfoil, there was considerable concern as to how the new shape would operate in actual flight. Therefore, the several U. S. government agencies responsible for aircraft, that is NASA, the Air Force, and the Navy, undertook a coordinated, three part flight demonstration program. The program was to evaluate the application of the new airfoil to a swept, long-range transport wing configuration, a thick wing, and a variable sweep fighter wing. In each case existing military aircraft were used as test beds. However, in none of the cases was it intended the test wing would be applied to production versions of these aircraft.

COMPARISON OF U.S. NAVY T-2C AIRPLANE WITHOUT & WITH THICK SUPERCRITICAL AIRFOIL

FIGURE 21

T-2C FLIGHT DEMONSTRATION PROGRAM

WING APPLICATION — M ≈ 0.8 AIRCRAFT

OBJECTIVE — INCREASED WING THICKNESS-TO-CHORD RATIO WITHOUT REDUCTION OF CRUISE MACH NUMBER

SPONSORS — U.S. NAVY & NASA

CONFIGURATION & STRUCTURAL DESIGN, FABRICATION, AND FLIGHT TESTS — NORTH AMERICAN-ROCKWELL, COLUMBUS, OHIO

CHRONOLOGY

APPROVAL — 1969
FIRST FLIGHT — 1970
COMPLETION — 1971

CONCLUSION — WIND-TUNNEL RESULTS VERIFIED

FIGURE 22

U.S. AIR FORCE F-111 WITH SUPERCRITICAL WING (TACT)

FIGURE 23

F-111 FLIGHT DEMONSTRATION PROGRAM (TACT)

WING APPLICATION — VARIABLE SWEEP FIGHTER

OBJECTIVE — IMPROVED MANEUVERABILITY & INCREASED CRUISE SPEED WITHOUT DEGRADATION OF OFF-DESIGN CHARACTERISTICS

SPONSORS — U.S. AIR FORCE & NASA

CONFIGURATION DESIGN & DEVELOPMENT — NASA LANGLEY & AMES

WING STRUCTURAL DESIGN & FABRICATION — GENERAL DYNAMICS

FLIGHT PROGRAM — NASA FLIGHT RESEARCH CENTER

CHRONOLOGY

APPROVAL — 1969
FIRST FLIGHT — 1973
COMPLETION — 1976

FIGURE 24

F-8

The transport supercritical wing configuration was flown on a Navy F-8 fighter (figure 19). The basic information concerning this program is given in figure 20. The wing was of simple "boiler plate" construction. Simple flaps extending from the 40% to the 80% semispan were used for both lateral control and increased lift for landing and take off. The sweep of the midchord was 40°. The airfoil shape outboard approximately the 40% semispan station was the same as that developed during the previously described two-dimensional investigations. However the airfoil shapes for the inboard section were substantially altered to account for the large three-dimensional effects in this region at the near sonic cruise Mach number. The forward extension of the leading edge near the fuselage also improved the near-sonic three-dimensional flow on this inboard region. The wing had substantial twist.

T-2C

The thick supercritical airfoil was flown on a Navy T-2C trainer. A comparison of aircraft without and with the thick section is shown in figure 21. The basic information concerning this program is given in figure 22. The section shape was obtained by drooping the flap and aileron and then adding balsa wood and fiberglass to the original wing structure. The airfoil shape was the same along the entire span. Some of the results from this program are present in reference 20.

F-111

The variable sweep supercritical fighter wing is being flown on a U. S. Air Force F-111 (figure 23). The basic information concerning this program is given in figure 24. Only the variable sweep panels have been changed from the original configuration. The wing panels have been designed for minimum weight and are equipped with single slotted trailing edge flaps and Kreuger leading edge flaps. The airfoil shapes are similar to those developed two-dimensionally. The panels have substantial twist.

VIII. Applications

Following the wind tunnel development of the near sonic transport wing configuration used for the F-8 flight demonstration, a complete near-sonic transport configuration, incorporating this wing was defined.[20] Three U. S. aircraft manufacturers,

ARTIST'S CONCEPT OF A NEAR-SONIC TRANSPORT INCORPORATING A SUPERCRITICAL WING

FIGURE 25

Boeing, General Dynamics, and Lockheed, under contract to NASA evaluated actual transport designs based on this configuration.[21] An artist's concept of the General Dynamic's design is shown in figure 25.

More recently a number of U. S. aircraft manufacturers have initiated new military and commercial airplane designs incorporating NASA supercritical airfoils. It should be noted that for transport aircraft the principal interest at present is in using the airfoils to obtain reduced fuel consumption rather than to obtain increased speed. For a given cruise speed the airfoils allow a reduction in wing sweep and/or an increase in section thickness ratio which permit an increase in wing aspect ratio or a reduction in wing weight. These changes of course provide a reduction in fuel consumption.

IX. Concluding Remarks

Over the past ten years extensive wind tunnel investigations of two-dimensional sections and three-dimensional applications of NASA supercritical airfoils have been conducted. In addition, two flight demonstration programs have been completed and another initiated. The results of this research indicate that the use of these airfoils can successfully provide substantial improvements of the speed, fuel consumption, or maneuverability of most aircraft intended for operation at high subsonic speeds. Also, the analytic methods now becoming available can greatly aid in the design of new operational aircraft incorporating these airfoils.

References

1. Stack, J.: Tests of Airfoils Designed to Delay the Compressibility Burble. NACA TN 976, 1944.

2. Abbott, I. H.; von Doenhoff, A. E.; and Stivers, L. S., Jr.: Summary of Airfoil Data. NACA Report No. 824, 1945.

3. Pearcey, H. H.: The Aerodynamic Design of Section Shapes for Swept Wings. Advances in Aeronautical Sciences, vol. 3, p 277. Pergamon Press, 1962.

4. Whitcomb, R. T.; and Clark, L. R.: An Airfoil Shape for Efficient Flight at Supercritical Mach Numbers. NASA TM X-1109, 1965.

5. Holder, D. W.: The Transonic Flow Past Two-Dimensional Aerofoils. J. Roy. Aeronaut. Soc., vol. 68, no. 644, Aug. 1964, pp. 501-516.

6. Bauer, F.; Garabedian, P. R.; and Korn, D. G.: Supercritical Wing Sections. Springer-Verlag, 1972.

7. Stratford, B. S.: The Prediction of Separation of the Turbulent Boundary Layer, J. Fluid Mech., vol. 5, pp. 1-16, 1959.

8. Loving, D. L.; and Katzoff, S.: The Fluorescent-Oil Film Method and Other Techniques for Boundary-Layer Flow Visualization. NASA Memo 3-17-59L, 1959.

9. Blackwell, J. A., Jr.: Preliminary Study of Effects of Reynolds Number and Boundary-Layer Transition Location on Shock-Induced Separation. NASA TN D-5003, 1969.

10. Van Dyke, M. D.; and Wibbert, G. A.: High-Speed Aerodynamic Characteristics of 12 Thin NACA 6-Series Airfoils. NACA MR A5F27, 1945.

11. Kacprzynski, J. J.; Ohman, L. H.; Garabedian, P. R.; and Korn, D. G.: Analysis of the Flow Past a Shockless Lifting Airfoil in Design and Off-Design Conditions. NRC Report LR-554, 1971.

12. Daley, N.; and Dick, S.: Effect of Thickness, Camber, and Thickness Distribution on Airfoil Characteristics at Mach Numbers Up to 1.0. NACA TN 3607, 1958.

13. Seddon, J.: The Flow Produced by Interaction of a Turbulent Boundary Layer With a Normal Shock Wave of Strength Sufficient to Cause Separation. R & M No. 3502, British A.R.C., March 1960.

14. Bavitz, P. C.: An Analysis Method for Two-Dimensional Transonic Viscous Flow, NASA TN D-7718, 1974.

15. Garabedian, P. R.; and Korn, D. G.: Analysis of Transonic Airfoils. Comm. on Pure and Applied Math., vol. 24, pp. 841-851, 1971.

16. Murman, E. M.; and Cole, J. D.: Calculation of Plane Steady Transonic Flows. AIAA J., vol. 9, No. 1, pp. 114-131, 1971.

17. Jameson, A.: Transonic Flow Calculations for Airfoils and Bodies of Revolution. Grumman Aero. Corp. Rep. 390-71-1, 1971.

18. Sells, C. C. L.: Plane Subcritical Flow Past a Lifting Aerofoil. Proc. Roy Soc. (London), vol. 308A, pp. 377-401, 1968.

19. Bradshaw, P.; Ferriss, D. H.; and Atwell, N. P.: Calculation of Boundary-Layer Development Using the Turbulent Energy Equation. J. Fluid Mech., vol. 28, part 3, pp. 593-616, 1967.

20. Ayers, T. G.: Supercritical Aerodynamics, Astronautics and Aeronautics, pp. 32-36, August 1972.

21. Braslow, A. L.; and Alford, W. J.: Advanced Subsonic Transport Technology. Astronautics and Aeronautics, pp. 26-31, August 1972.

Symbols

c	chord of airfoil
c_d	section drag coefficient
c_m	section moment coefficient
c_n	section normal force coefficient
C_p	pressure coefficient $C_p = \frac{P(\text{local})-P(\text{ambient})}{q}$
M	Mach number
p	pressure
q	dynamic pressure
t	airfoil thickness
x	distance from leading edge of airfoil
z	vertical dimension from horizontal reference
α	angle of attack